J Mater Sci (2010) 45:5851–5859
DOI 10.1007/s10853-010-4661-7

Effect of filler dispersion degree on the Joule heating stimulated recovery behaviour of nanocomposites

**H. H. Le · I. Kolesov · Z. Ali · M. Uthardt ·
O. Osazuwa · S. Ilisch · H.-J. Radusch**

Received: 8 January 2010 / Accepted: 26 May 2010

Abstract Composites based on highly branched ethylene-1-octene copolymer (EOC) and carbon black (CB) with different dispersion degree of CB were prepared. The method of the online measured electrical conductance/resistance was used to monitor the change of the electrical conductance/resistance of the composites during the preparation processes, i.e. mixing and cross-linking. It was found that the kinetics of thermally stimulated shape-memory recovery of CB filled EOC is strongly influenced by the filler dispersion degree, which actually affects the heat transfer in the composites. Using a special arrangement of experiments the Joule heating stimulated shape-memory behaviour was quantified. CB dispersion degree and related electrical resistivity determine the extent of the Joule heating stimulated shape-memory behaviour. Composite collected at the maximum in the online measured conductance–time characteristics showed the best shape-memory effect owing to the highest electrical conductivity in the solid state. The CB filled EOC showed a negative thermal coefficient of resistivity (NTC) effect, which accelerates the temperature increase and shape-memory recovery of the composites when applying a voltage.

Introduction

Shape-memory polymers are a definite type of actively moving polymers. For distinct appearance of the thermally induced shape-memory effect the existence of a stable physically or covalently crosslinked network and a thermal transition (e.g. melting or glass transition) at convenient temperatures, T_{trans}, are essential [1–3]. For covalently crosslinked semi-crystalline polymers, e.g. in the case of peroxide cross-linking, a shape-memory behaviour with high performance can be achieved if the following requirements are fulfilled. First, the polymeric material must possess a thermally and mechanically resistant network with suitable high cross-linking density in order to produce sufficiently strong elastic and viscoelastic forces under load at programming temperature $T_{\text{pr}} > T_{\text{trans}}$ and preferably minimal residual strain. Furthermore, a sufficient strain at failure of the polymer network is necessary. Second, the crystalline phase formed after cooling of the loaded sample must be able to fix the strain and the elastic/viscoelastic forces stored in the network efficiently. With the exception of polyconjugated polymers, polymers are not intrinsically conductive. However, by compounding with conductive fillers or blending with intrinsically electrically conductive polymer these compounds/blends become conductive. By applying a voltage the conductive polymer compounds can be internally heated due to the release of Joule energy and in the case of shape-memory polymers their thermally induced shape-memory effect will be stimulated indirectly. A meaningful review of literature on particle filled shape-memory polymers can be found in [4, 5]. Generally, a good recovery could be maintained for filled shape-memory polymers when keeping low both the electrical resistivity and stiffness. With increasing filler loading the electrical resistivity decreases, however, the stiffness increases that deteriorates significantly the shape-memory behaviour. Many attempts have been done in order to overcome such problems, e.g. Lan et al. [6] proposed a fabrication of shape-memory polyurethanes, which have anisotropic electro-thermo-mechanical

---

H. H. Le (✉) · I. Kolesov · Z. Ali · M. Uthardt · O. Osazuwa ·
S. Ilisch · H.-J. Radusch
Center of Engineering Sciences, Polymer Technology,
Martin Luther University Halle-Wittenberg, Kurt-Mothes-Str. 1,
06099 Halle, Germany
e-mail: hai.le.hong@iw.uni-halle.de

properties by orientating nickel powder in molten polyurethanes by applying a magnetic field. Leng et al. [7] prepared high conductive nanocomposites containing a hybrid filler system of conductive carbon black (CB) and carbon fibre (CF). It was discussed that the particulate additives are dispersed homogeneously within the matrix and serve as interconnections between the CF, while the fibrous additives act as long distance charge transporter by forming local conductive paths. Several authors [8–12] achieved high conductivity by incorporating a small amount of carbon nanotubes into the shape-memory polymers. Another simple possibility to control the conductivity and hardness is to vary the degree of filler dispersion. Depending on the material parameters and mixing technology CB undergoes different dispersion states, i.e. from large agglomerates to small aggregates [13]. In order to obtain optimal vulcanizate properties CB must be sufficiently dispersed in the mixture [14–18]. The degree of filler dispersion can be monitored and controlled directly during the mixing process using the online measured electrical conductance (OMEC) [19, 20]. A close correlation between the OMEC, the dispersion degree and mechanical properties like stress–strain characteristics [21], stress relaxation behaviour [22] or electrical resistivity [18] has been found.

Recently, thermally induced shape-memory polymers based on peroxidic cross-linked ethylene-1-octene copolymer (EOC) have been developed [23, 24]. Systematic investigations of the relation between shape-memory behaviour and characteristics of the covalent network and the crystalline structure of EOC were performed [23]. Blends of EOC with polyethylene (HDPE) having an especially fine disperse and distinctly segregated phase morphology exhibited a multiple shape-memory behaviour [24]. Obviously, that is caused by multiple melting behaviour of these blends with several poorly separated peaks. Addition of CB into EOC reinforces the polymer and imparts high electrical conductivity. The Joule heating stimulated shape-memory effect of EOC filled with different CB types and concentrations has been systematically investigated in [25]. In the present work, the effect of the degree of CB dispersion, which can be controlled by the OMEC, on the shape-memory behaviour of EOC will be characterized and discussed by taking into account the extent of the electrical properties and rigidity of the CB network of the composites.

Experimental

Materials and composite preparation

Metallocene-catalyzed homogeneous EOC (Dow Chemical) with approximately 60 hexyl branches per 1,000 carbon atoms, a mass-average molecular weight M_w of 87 kg/mol and a polydispersity M_w/M_n of 2.5 was used as matrix. As cross-linking agent 2,5-dimethyl-2,5-di-(*tert*.butylperoxy)-hexane (DHBP) (Evonik) was used. A high conductive CB EC600 (Akzo Nobel Chemicals) was used as filler. Its structural parameters, dibutylphthalat number (DBP) of 500 ml/100 g and nitrogen surface area (NSA) of 1,400 m^2/g, were given by the provider.

Preparation of the composites was performed in a Poly Lab System Rheocord 300 p with a 75 cm^3 mixing chamber Rheomix 610 p (Thermo Haake). The initial chamber wall temperature was kept constant at 60 °C, the rotor speed 50 rpm, and the fill factor 0.7. First, EOC and peroxide were mixed for 2 min and then CB was added at 5 min mixing time. A peroxide concentration of 2.5 wt% and CB content of 17 wt% were kept constant for all composites. Composites with different mixing times were prepared in order to obtain different degrees of CB dispersion. The choice of mixing time was based on the OMEC-mixing time characteristics as described in our previous work [26]. Three samples nominated as E-9m, E-20m and E-35m were prepared with the mixing time of 9, 20 and 35 min. An unfilled cross-linked EOC was prepared as reference sample E0.

After mixing, the mixture was processed to a thin plate by a compression moulding device with a thickness of 0.5 mm at 130 °C and immediately cross-linked at a temperature of 190 °C. The cross-linking time at 190 °C was determined using a vulcameter Elastograph (Göttfert Werkstoff-Prüfmaschinen).

Optical microscopy

Optical microscopy has been used to characterize the macrodispersion of CB. This method was first described by Stumpe and Railsback [27] and modified by us [19]. Glossy cuts were produced by cutting the stretched samples by a razor blade at room temperature. The cut area was analysed by optical microscopy in reflection mode using a Leica RM-DX (Leica). If the surface of a cut contains CB agglomerates or aggregates, the light is scattered at this place and its area appears dark. With an image analysis program the area of visible CB regions was quantified. The degree of the macrodispersion was assessed as the ratio of the amount of the non-dispersed agglomerates with an average diameter larger than 6 μm to the total surface. A dispersion index of 100% means that no agglomerate larger than 6 μm could be found in the cut area. From every sample six images were taken and from each picture six image analyses were evaluated.

Atomic force microscopy

Morphological investigations were carried out by an atomic force microscope Q-Scope 250 (Quesant) operated in intermittent mode. Samples were produced by cutting in a cryo-chamber CN 30 (Microm) with a diamond knife at −150 °C.

Electrical resistivity measurement

For electrical resistivity measurements of the samples a multimeter 2750 (Keithley) was used. The shape of the conductive test specimen was a rectangular strip with length of 50 mm and the cross-section area of $5 \times 0.5\ \text{mm}^2$. The ends of specimens were coated by silver paste in order to receive a good contact with the two electrodes.

Mechanical testing

Tensile tests were carried out according to EN ISO 527 at room temperature and with a crosshead speed of 200 mm/min using an universal tensile test machine 1425 (Zwick/Roell). Six samples were tested for all composites produced.

Dynamic mechanical analysis

Dynamic mechanical behaviour was characterized using a dynamic mechanical analyser Qualimeter Eplexor 500 N (Gabo) in tensile mode at a frequency of 1 Hz at different temperatures ($20\ ^\circ\text{C} < T < 170\ ^\circ\text{C}$) with a heating rate of 1 K/min.

Development of sample temperature by applying a voltage

Upon application of an electrical voltage, the sample temperature is increased as a result of the Joule effect. For the characterization of the temperature development samples with the dimensions $l \times w \times d$ of $40 \times 10 \times 0.5\ \text{mm}^3$ were cut from the cross-linked compression-moulded plate. Along the length l both edges of the sample were coated with silver paste in order to get good contact between sample and voltage source. The temperature of the sample was measured using a non-contact temperature measuring device MiniTemp (Neo-Lab).

Characterization of the shape-memory behaviour in bending test

Samples prepared for the shape-memory experiments had dimensions of $40 \times 10 \times 0.5\ \text{mm}^3$ ($l \times w \times d$). The shape-memory experiments were performed in bending mode. The samples were wrapped round a metal tube having an outer diameter $D = l/\pi$, and fixed by an insulating tape. The wrapped samples were then brought into an oven, which was heated up to the programming temperature (T_{pr}) of 90 °C. After 5 min annealing in oven the samples were quenched in cool water of 20 °C to fix their shape. Using this time and temperature controlled preparation procedure the ring-like shaped samples are obtained and they are ready for subsequent shape-memory experiments.

When the strip is deformed to a ring, the inner layer of the ring is compressed, whereas the outer layer is stretched with a deformation $\varepsilon = d\pi/l = 3.93\%$.

For thermally stimulated shape-memory experiments the programmed samples were fixed on an isolating ground with an insulating tape and inserted into a pre-heated oven of 90 °C. Photographs of the samples were taken along the recovery time. In order to characterize the effect of temperature on the shape-memory behaviour, oven temperature was increased continuously with a heating rate of 1 K/min.

For the characterization of the Joule heating stimulated shape-memory behaviour the programmed samples were fixed on an isolating ground by two clamps as described in [25] and shown in Fig. 1a. The clamps were connected with a voltage source, and a voltage of 10 V was applied. The resulting current and the induced temperature of the specimen depend on the electrical resistance of the composite. During heating the ring opens and deforms to the permanent shape of a rectangular strip as seen in Fig. 1b.

In order to quantify the recovery, r, the change of the contour of the sample during heating was analysed using Eq. 1 [25].

$$r = \frac{\varphi - \varphi_0}{180^\circ - \varphi_0} \times 100\% \qquad (1)$$

φ_0 is the initial angle determined after programming (Fig. 1a). φ_0 characterizes the ability of the composite to fix the temporary shape of the sample. If the crystalline phase of the sample formed during quenching in cool water is strong enough to fix the deformation efficiently, φ_0 is zero. Otherwise, φ_0 has a certain value, which is determined by the programming temperature and the cross-linking density of EOC as well as the rigidity of the CB network. φ is the angle describing the opening process during heating. A 100% recovery is reached when φ reaches 180°.

For the recovery test at least three measurements were performed to get a sufficient statistics of measured values.

Results and discussion

CB dispersion and electrical conductivity

Online conductance curves of the composites E-9m, E-20m and E-35 m recorded during the mixing process are

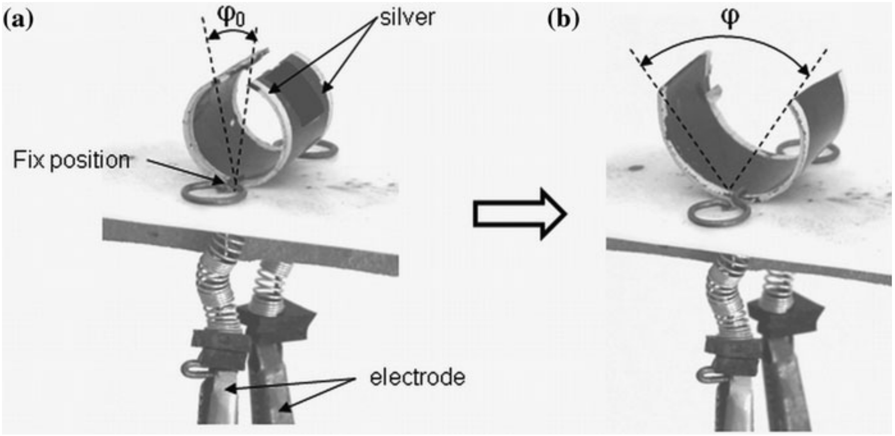

Fig. 1 Arrangement of the Joule heating stimulated SM experiment and quantification of the SM behaviour by analysis of the sample contour

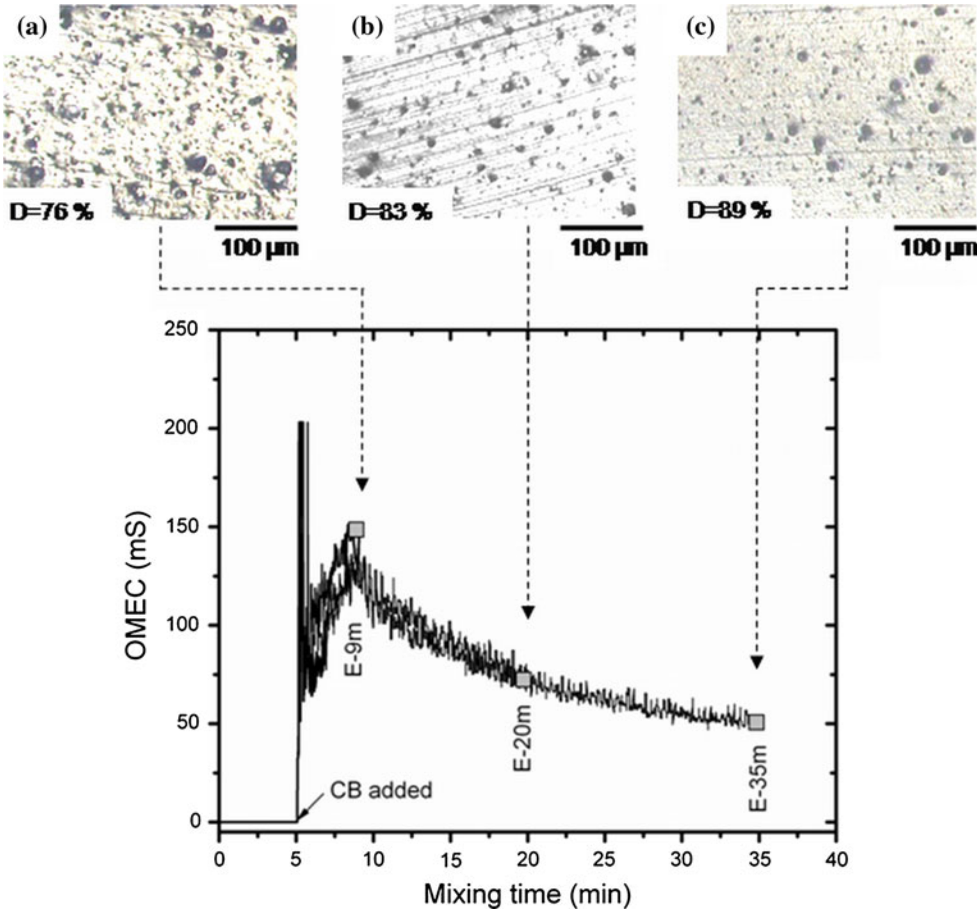

Fig. 2 OMEC of the composites E-9m, E-20m and E-35m

presented in Fig. 2. The curves show the typical shape as received in our previous works [19, 20, 26]. They overlap each other that indicates a very good reproducibility of the mixing process. The minimum of the conductance curves is observed at about 6 min and the local maximum named BIT (black incorporation time) at 9 min. The CB agglomerates undergo the largest change of the size in the range between the minimum and maximum value of conductance.

After passing the local maximum the conductance decays rapidly but the macrodispersion still increases slightly. Figure 2a–c shows the morphology of the composites made by optical microscopy at different mixing times. Several CB agglomerates can be observed in the images. The macrodispersion degree, *D*, describing the change of the CB agglomerate size was determined from the images. As discussed in our previous work [19, 20, 26] the main reason for the decrease of conductance after BIT

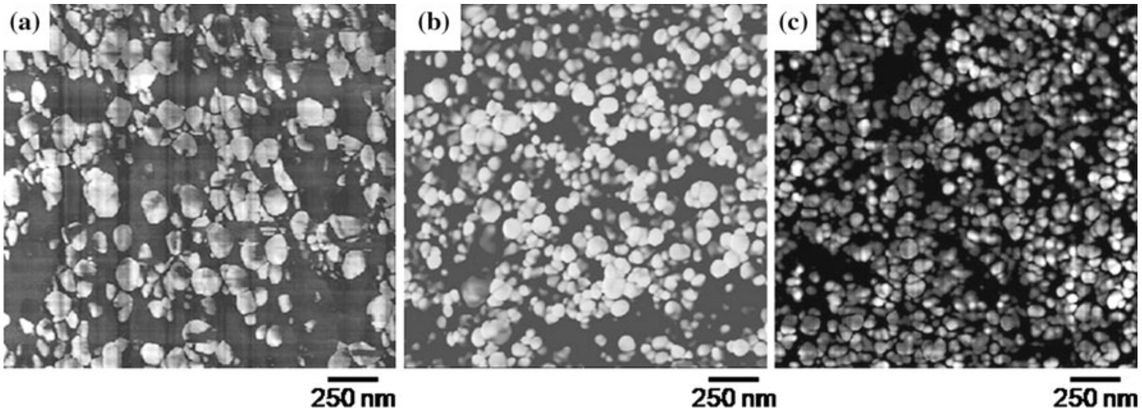

Fig. 3 AFM images of E-9m (**a**), E-20m (**b**) and E-35m (**c**)

is related to the better distribution of small aggregates throughout the matrix, which can be described by the microdispersion.

In the AFM image of sample E-9m (Fig. 3a) the small aggregates and the remaining agglomerates (light domains) build a strong continuous network in the EOC matrix (dark regions). This strong network facilitates the motion of electrons and thus the online conductance increases up to a local maximum. Some large unfilled regions can be observed in sample E-9m because of an insufficient distribution process. After 9 min, the macrodispersion processes slow down as seen in Fig. 2 while the microdispersion processes continue. The size of agglomerates and aggregates reduces with the mixing time as seen in Fig. 3b, c. Furthermore, in Fig. 3b, c a better distribution of small aggregates throughout the matrix is observed that weakens the CB network and causes a decay of the OMEC in this period. The large unfilled regions seem to disappear in sample E-20m and E-35m.

Figure 4 shows that the specific resistivity changes correspondingly to the OMEC. Because the specific resistivity is measured for definite sample geometry by keeping the temperature constant, the CB network in the sample is in a steady state during the measurement. Further, for the measurement of the specific resistivity the sample must be vulcanised. During the vulcanisation process under high temperature and pressure, some reformation of the CB network due to the migration process of CB aggregates takes place affecting the resistivity of the vulcanisates [28]. In contrast, the online conductance measured directly in the mixing chamber depends on the equilibrium number of the contacts of the small CB aggregates which undergo permanent motion during the mixing. However, the correlation between the online conductance and specific resistivity is displayed in Fig. 4.

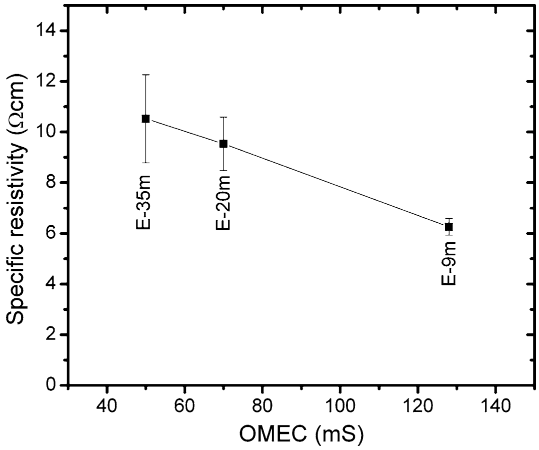

Fig. 4 Correlation between OMEC and specific resistivity

Mechanical properties

Typical stress–strain curves for the samples investigated at room temperature are shown in Fig. 5a. The curves show nearly the same shape. However, the elongation at break of sample E-20m is higher compared to the other samples because of the good CB macrodispersion. Sample E-35m shows a very good CB macrodispersion, but after longer mixing time EOC molecules may be damaged, influencing the elongation of the sample.

In Fig. 5b, the temperature dependence of the storage modulus *E*′ obtained from dynamic mechanical analysis is presented. It is obvious that the degree of CB dispersion has only a weak effect on the progress of the storage modulus. The storage modulus *E*′ decreases rapidly in the temperature range up to 70 °C. In this range, the processed melting of the crystalline EOC phase is responsible for the strong decrease of the storage modulus [25]. In the temperature range above 70 °C the storage modulus decays, however, with lower rate. Based on the systematic

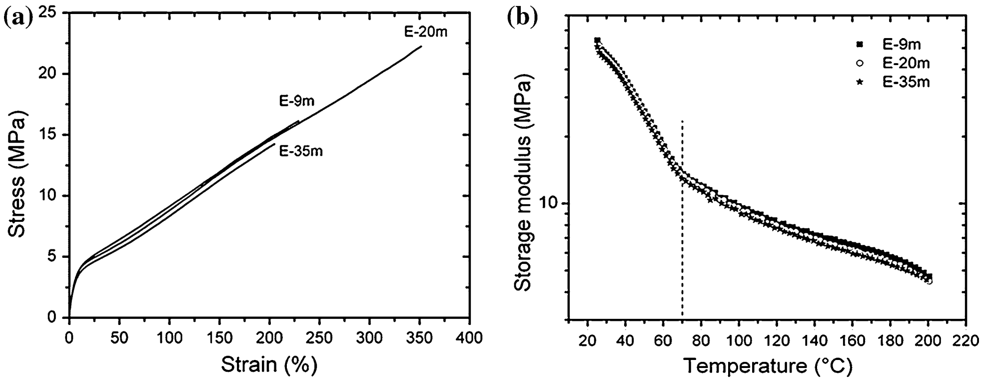

Fig. 5 Stress–strain behaviour at room temperature (**a**) and storage modulus in dependence on the test temperature (**b**) of the composites E-9m, E-20m and E-35m

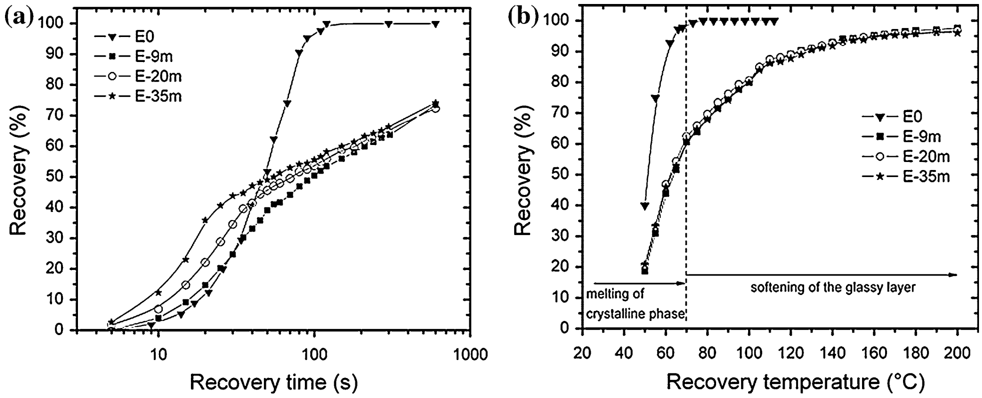

Fig. 6 Recovery at 90 °C in oven in dependence on the recovery time (**a**), recovery at different temperatures (**b**)

investigation using stress relaxation experiment for CB filled vulcanisates [22] the physical background of the temperature dependence of E-modulus at temperatures higher than 70 °C was discussed. It was explained that the debonding of the rubber-layer from the CB surface and the collapse of a part of the CB network are responsible for the decrease of E-modulus in this temperature range. According to the model of flexible chain aggregates [29] the main contribution of the elastic energy in the strained filler clusters results from the bending–twisting deformation of filler–filler bonds. The typical non-linear viscoelastic behaviour of reinforced rubbers with pronounced stress softening and hysteresis results mainly from the breakdown and re-aggregation of the filler network at large strain amplitudes [30].

Thermally stimulated shape-memory behaviour

Figure 6a shows the shape-memory recovery of the composites and the unfilled sample E0 investigated in an oven at 90 °C in dependence on the recovery time. E0 recovers in the first period very slowly and then very fast in the second period. After 100 s a complete recovery was obtained. According to our previous works [24, 25], E0 is a semi-crystalline shape-memory polymer with covalent network. Below the melting temperature, $T_m = 70$ °C, the cross-linked EOC is characterized by two different three-dimensional networks: the chemical network consisting of chemical cross-links and the crystalline network. Above T_m the crystalline phase melts and only the chemical cross-links remain, thus EOC will recover to its permanent shape under the effect of entropy forces of the deformed chemically cross-linked network.

It is obvious that in the short time range up to 10 s samples recover slowly because they need time to be heat-soaked. Composites with higher CB dispersion degree recover faster than those with lower dispersion degree and the unfilled sample E0. That is related to the assumption that the heat transfer becomes more effective with higher degree of CB dispersion. In the composite with lower dispersion degree like sample E-9m some large unfilled regions are still available as seen in Fig. 3, and they hinder the heat transfer between the filled regions. In the longer time range, when the composites are heated thoroughly, the recovery becomes similar for all composites independent of the dispersion degree. Although after 100 s, E0 is recovered completely, the composites do not reach an end-value of recovery even after 300 s. The investigated composites show a much lower recovery compared to E0 that is related to the rigid CB network, which deteriorates the recovery process.

The effect of oven temperature on the recovery is presented in Fig. 6b in the range between 50 and 200 °C. As expected the recovery increases rapidly when the temperature increases in the range up to 70 °C. According to previous DSC investigation [25], up to 70 °C the crystalline phase, which prevents the recovery process, melts totally. Above 70 °C the crystalline phase is no more available, and as a result, E0 reaches a recovery of nearly 100%. In comparison to this behaviour the composites show a lower recovery at 70 °C. With further increasing temperature the recovery of the composites slowly increases. Based on the entropy-elasticity theory when the temperature changes from 70 to 200 °C, an increase of the entropy-elastic modulus of the EOC matrix, and thus the entropy-elastic stress, of about 38% was calculated. This temperature dependent increase of the entropy-elastic stress is the one reason for a better recovery of the composites at 200 °C. Another reason for a better recovery of the composites at temperatures higher than 70 °C may be related to the temperature dependent rigidity of the CB network. As mentioned above, at a filler concentration above the percolation threshold, the CB aggregates are connected together by a thin polymer layer forming a continuous network. The investigated composites show relatively low values of electrical resistivity, because of the possibility that the electrons can move by jumping across the gap between two aggregates or by the electron tunnelling effect.

Using 3D-TEM technique, Kohjiya et al. [31] calculated that in such a conductive network the polymer layer has different thickness which lies in the order of about 1.0–3.0 nm. According to independent investigations made by several authors [32–35], in close vicinity to the CB surface within 1.0–1.5 nm, the molecular mobility of the polymer layer is extremely restricted due to the interaction with the CB surface. The immobilized polymer layer holds the CB network rigid to resist the recovery forces. The rigidity of the network is characterized by a specific glass temperature of the immobilized layer T_G^{il}. If the T_G^{il} is exceeded, the immobilized layer becomes mobile, and the network looses its reinforcement effect. The softening of the immobilized polymer layer and the related break-up of the CB network is the reason for the decrease of E-modulus as seen in Fig. 5b. According to nuclear magnetic resonance (NMR) investigations, Kaufman et al. [32] determined T_G^{il} of about 100 °C for CB filled ethylene propylene rubber (EPDM). By use of the thermally scanning stress relaxation (TSSR) on filled elastomers Srinivasan et al. [36] found that an increase of the temperature above 120 °C would further aid in weakening filler–filler bonds. According to previous results [22], at temperatures higher than 70 °C the collapse of the bending–twisting deformed filler–filler bonds in CB filled acrylonitrile butadiene rubber (NBR) was supposed as a new relaxation process. Softening of the filler network at 90 °C was also observed in CB filled PP/EPDM-TPE using stress relaxation measurements [37]. In Fig. 6b, the recovery of the composites approaches similarly the value of E0 when the temperature increases to 200 °C. Despite the different macro- and microdispersion degree the macroscopic properties like temperature dependent shape-memory recovery are similar for the composites investigated. The reason is that the number and thickness of the immobilized polymer layers of the CB networks do not differ so much from each other.

Joule heating stimulated shape-memory behaviour

The Joule heating stimulated shape-memory experiments of the composites investigated were carried out by applying a voltage of 10 V. Images presented in Fig. 7a were taken along the recovery time. The value of recovery was quantified using Eq. 1. The results are presented in Fig. 7b in dependence on the recovery time. It is obvious that the rings opened with different rate and extent. The composite E-9m shows the best shape-memory behaviour and E-35m the worst one. After 300 s the recovery of E-9m, E-20m and E-35m was measured with values of 90%, 80% and 59%, respectively.

In order to evaluate the different shape-memory behaviour of the composites, the sample temperature, T, and electrical conductance, $1/R$, were recorded during the

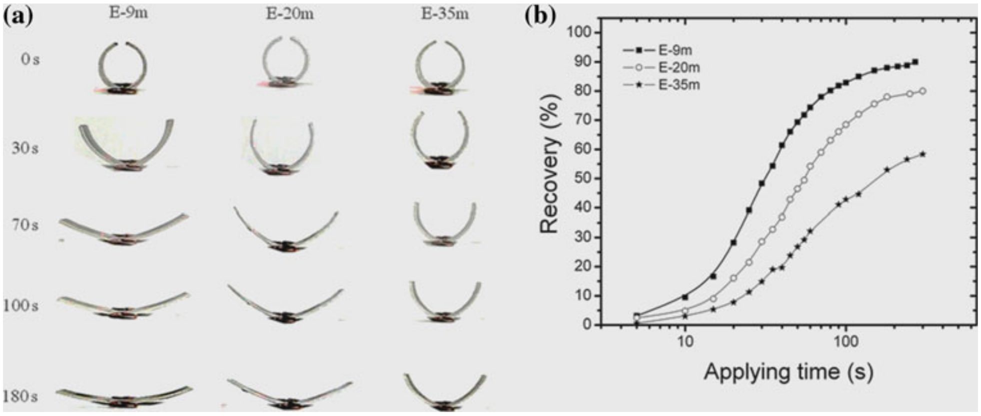

Fig. 7 Time dependent change of the sample contour (**a**) and recovery (**b**) of composites E-9m, E-20m and E-35m by application of 10 V

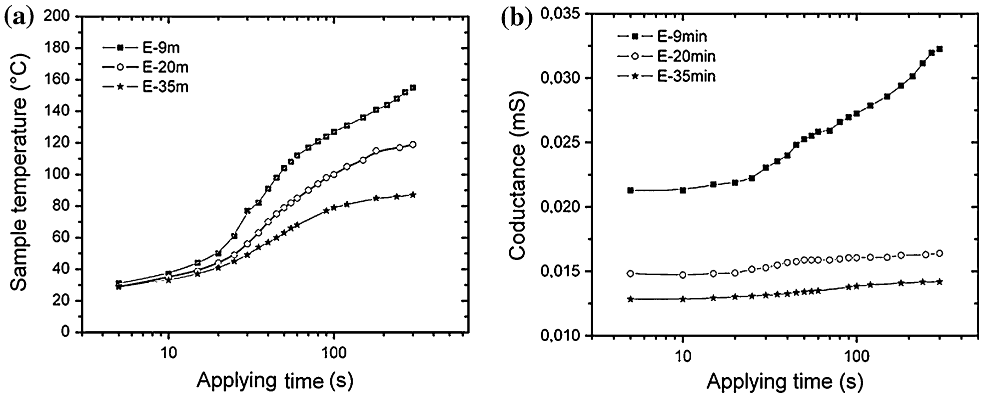

Fig. 8 Sample temperature (**a**) and conductance (**b**) of E-9m, E-20m and E-35m by application of 10 V in dependence on applying time

shape-memory experiment. The development of the sample temperature of E-9m, E-20m and E-35m by applying 10 V is presented in Fig. 8a. After a delay time of about 20 s the surface temperature of the composites increases rapidly. After 300 s a sample temperature of 156, 118 and 85 °C was achieved for E-9m, E-20m and E-35m, respectively.

Figure 8b shows that the conductance, $1/R$, of the composites increases with the applying time, t, as a result of the increase of sample temperature, T. This means that the investigated composites show a negative temperature coefficient (NTC) of resistivity, whereas the resistivity increase upon increasing temperature is described by a positive temperature coefficient (PTC) [38–40]. Crystalline polymers usually show PTC effects where an abrupt increase of resistivity is observed near the melting point of the polymer matrix [40]. According to Voet [41], the thermal expansion of the polymer layer connecting the CB aggregates is assumed to be the reason for the PTC effect. It should be noted that the NTC effect is only slightly distinct at the samples with high CB dispersion degree and only sample E-9m exhibits an evident increase of conductance or decrease of resistivity, respectively, with increasing temperature in the range above the melting temperature of the polymer used (see Fig. 8). In this temperature range the mobility of the polymer segments increases owing to the fusion of crystalline domains and the flocculation of the CB network is preferably generated, thus the conductivity increases. The described behaviour and their explanation are consistent with results of Das et al. [42] received for EVA and especially for amorphous EPDM. Concentration and properties of CB, especially the particle size, are of importance to the temperature characteristics of conductivity of CB filled rubbers [43]. Proper high concentration and large particle size of CB lead to the PTC effect, whereas small particle sizes and low concentrations of CBs lead to the NTC effect. In the present work, the used CB is a high conductive one with very small particle size. Only NTC effect was observed for different CB dispersion degree. The extent of the increase of conductivity after a certain applying time is caused by different induced sample temperature.

Assuming a simple relation between applied voltage, U, sample temperature, T, and conductance, $1/R$, the energy-conversion efficiency, k, can be evaluated according to Eq. 2 as ratio between the heat needed for heating up to temperature T and Joule's heat

$$k = \frac{m \int_{T_\mathrm{R}}^{T} c_\mathrm{p}^\mathrm{ap} \mathrm{d}T}{U^2 \int_0^t \frac{1}{R} \mathrm{d}t} \tag{2}$$

where m denotes the mass of the samples, c_p^ap is the apparently specific heat capacity, U is the applied voltage and T_R is the room temperature.

T was determined from Fig. 8a at an applying time $t = 300$ s. c_p^ap was determined from DSC experiments by taking into consideration data for polyethylene taken from the advanced thermal analysis system (ATHAS). An energy-conversion efficiency, k, of 6.8%, 9.0% and 7.4% was calculated for E-9m, E-20m and E-35m. That corresponds to the 10% efficiency received for filled polyurethanes [8], under the simple assumption that c_p and $1/R$ are independent of temperature.

Conclusions

Joule heating stimulated and thermally induced shape-memory behaviour of crosslinked ethylene-1-octene copolymer filled with CB has been investigated in bending mode by relatively low local deformation below 4% under special consideration of the effect of filler dispersion degree. Melt mixing supported by the method of the OMEC was used to prepare CB filled shape-memory polymers based on peroxide crosslinked ethylene-1-octene copolymer with different degree of CB dispersion. Kinetics of thermally stimulated shape-memory recovery is strongly influenced by the CB dispersion degree, which actually improves the heat transfer in the composites. The increasing degree of CB dispersion and related electrical resistivity impair the Joule heating stimulated shape-memory behaviour. CB filled EOC shows a NTC effect, which in turn accelerates the temperature increase and shape-memory recovery of the composites when applying a voltage. An energy-conversion efficiency *k* describing the usage efficiency of Joule's heat for sample heating to desired temperature amounts 7–9%.

References

1. Lendlein A, Langer R (2002) Science 296:1673
2. Lendlein A, Kelch S (2002) Angew Chem Int Ed 41:2034
3. Behl M, Lendlein A (2007) Mater Today 10:20
4. Gunes IS, Cao F, Jana SC (2008) Polymer 49:2223
5. Gunes IS, Jana SC (2008) J Nanosci Nanotechnol 8:1616
6. Lan X, Huang WM, Leng JS, Liu N, Phee LSJ, Yuan Q (2008) Gummi Fasern Kunstst 61:784
7. Leng J, Liu HL, Liu Y, Du S (2007) Appl Phys Lett 91:144105-1
8. Cho JW, Kim JW, Jung YC, Goo NS (2005) Macromol Rapid Commun 26:412
9. Paik IH, Goo NS, Jung YC, Cho JW (2006) Smart Mater Struct 15:1476
10. Jiang X, Bin Y, Matsuo M (2005) Polymer 46:7418
11. Ni QQ, Zhang Ch, Fu Y, Dai G, Kimura T (2007) Compos Struct 81:176
12. Meng Q, Hu J, Zhu Y (2007) J Appl Polym Sci 106:837
13. Heinrich G, Klüppel M, Vilgis TA (2002) Curr Opinion Solid State Mater Sci 6:195
14. Takino H, Iwama S, Yamada Y (1997) Rubber Chem Technol 70:15
15. Hess WM, Chirico VE (1997) Rubber Chem Technol 50:301
16. Hess WM, Scott CE, Callan JE (1967) Rubber Chem Technol 40:371
17. Schuster RH, Meier J, Klüppel M (2000) Kautsch Gummi Kunstst 53:663
18. Le HH, Tiwari M, Ilisch S, Radusch H-J (2006) Plast Rubber Compos Macromol Eng 35:410
19. Le HH, Ilisch S, Jakob B, Radusch HJ (2004) Rubber Chem Technol 77:147
20. Le HH, Ilisch S, Steinberger H, Radusch H-J (2008) Plast Rubber Compos Macromol Eng 37:367
21. Ali Z, Le HH, Ilisch S, Busse K, Radusch H-J (2009) J Appl Polym Sci 113:667
22. Le HH, Ilisch S, Radusch H-J (2009) Polymer 50:2294
23. Kolesov IS, Kratz K, Lendlein A, Radusch H-J (2009) Polymer 50:5490
24. Kolesov IS, Radusch H-J (2008) eXPRESS Polym Lett 2:461
25. Le HH, Ilisch S, Radusch H-J (2010) Electrically stimulatable shape-memory materials based on carbon black filled ethylene-octene copolymer (EOC) and their blends. 10th European symposium on polymer blends, March 7–10, 2010. Dresden, Germany, Book of abstracts, p. 94
26. Le HH, Tiwari M, Ilisch S, Radusch H-J (2005) Kautsch Gummi Kunstst 58:575
27. Stumpe NA, Railsback HE (1964) Rubber World 151:41
28. Zhang J, Feng S (2003) J Appl Polym Sci 89:3471
29. Kantor Y, Webman I (1984) Phys Rev Lett 52:1891
30. Klüppel M (2003) Adv Polym Sci 164:1
31. Kohjiya S, Katoh A, Suda T, Shimanuki J, Ikeda Y (2006) Polymer 47:3298
32. Kaufman S, Slichter WP, Davis DD (1971) J Polym Sci A 9:829
33. Vieweg S, Unger R, Hempel E, Donth EJ (1998) Non-Cryst Solids 235:470
34. Arrighi V, Higgins JS, Burgess AN, Floudas G (1998) Polymer 39:6369
35. Litvinov VM, Spiess HW (1991) Makromol Chem 192:3005
36. Srinivasan N, Bökamp K, Vennemann N (2005) Kautsch Gummi Kunstst 58:650
37. Le HH, Heidenreich D, Kolesov IS, Ilisch S, Radusch H-J (2009) J Appl Polym Sci. doi:30769
38. Tang H, Piao JH, Yang HL (1993) J Appl Polym Sci 48:1795
39. Klason C, Kubat J (1975) J Appl Polym Sci 19:831
40. Narkis M, Ram A, Flashner F (1978) Polym Eng Sci 18:649
41. Voet A (1981) Rubber Chem Technol 54:42
42. Das NC, Chaki TK, Khastgir D (2003) J Appl Polym Sci 90:2073
43. Zhang J, Feng S (2003) J Appl Polym Sci 90:3889